Int. J. Exp. Path. (2007), 88, 351–360
doi: 10.1111/j.1365-2613.2007.00539.x

ORIGINAL ARTICLE

The mouse mammary carcinoma 4T1: characterization of the cellular landscape of primary tumours and metastatic tumour foci

Sally A. DuPré*, Doug Redelman† and Kenneth W. Hunter, Jr*

*Department of Microbiology and Immunology and †Department of Physiology and Cell Biology, University of Nevada School of Medicine, Reno, NV, USA

INTERNATIONAL JOURNAL OF EXPERIMENTAL PATHOLOGY

Received for publication:
19 March 2007
Accepted for publication:
23 April 2007

Correspondence:
Dr Sally A. DuPré
Department of Microbiology and Immunology
University of Nevada School of Medicine
1664 North Virginia Street
Reno, NV 89557-032, USA
Tel.: 775-784-7064
Fax: 775-327-2332
Email: sdupre@unr.nevada.edu

Summary

The murine mammary carcinoma 4T1 causes a leukemoid reaction with profound granulocytosis coincident with the production of tumour-derived growth factors. Here, we study the evolving cellular landscape of primary tumours and metastatic tumour foci and correlate haematopoietic cell infiltration with the production of tumour-derived chemokines. Flow cytometric analysis of enzyme digested primary tumours at different times after transplantation revealed a progressively increasing $CD45^+$ haematopoietic cell infiltrate consisting predominantly of $CD11b^+$ myeloid cells. Most of these cells had an $F4/80^+/CD11c^+$ phenotype, many of which also stained $Gr\text{-}1^+$. Smaller numbers of $Gr\text{-}1^+CD11b^+$ granulocytes and lymphoid cells were also identified. Progressive increases in $Gr\text{-}1^+$ granulocytes were observed in enzymatic digests of livers and lungs with metastatic tumour foci. Cultured 4T1 tumour cells expressed mRNA transcripts for the myeloid cell chemokines RANTES, MCP-1 and KC, and enzymatically digested cells from primary 4T1 tumours partially depleted of $CD45^+$ cells expressed transcripts for these chemokines and also MIP-1α and MIP-1β. These data demonstrate that 4T1 tumour-bearing mice have mixed myeloid cell infiltrates of primary tumours and granulocytic infiltrates of metastatic organs. This pathologic presentation correlated with the expression of tumour-derived chemokines.

Keywords
4T1, carcinoma, chemokines, infiltrates, mammary

Myeloid cells play a protective role in some tumours by participating in antibody-dependent cell-mediated tumour cytotoxicity (Di Carlo *et al.* 2001), and enhancing myeloid infiltration of primary tumours with cytokines and growth factors has led to tumour remission (Colombo *et al.* 1991, 1996). On the other hand, it has been shown that myeloid cells may actually contribute to tumour growth and metastasis (Aeed *et al.* 1988; Welch *et al.* 1989; Coussens & Werb 2001; Wu *et al.* 2001; Borsig *et al.* 2002), and depletion of myeloid cells has promoted tumour remission in some human and animal tumours (Tabuchi *et al.* 1992; Pekarek *et al.* 1995). Recently, tumour-infiltrating $Gr\text{-}1^+CD11b^+$ cells have been characterized as myeloid suppressor cells capable of inhibiting specific T-cell-mediated tumour immunity (Bronte *et al.* 1998; Bronte *et al.* 2001 Almand *et al.* 2001; Kusmartsev & Gabrilovich 2002; Serafini *et al.* 2004). It

seems that myeloid cells represent the proverbial double-edged sword in tumour biology, and a more thorough study of these cells is warranted, particularly in tumours where myelopoiesis is a prominent feature.

The mouse mammary carcinoma 4T1 was originally isolated as subpopulation 410.4 derived from a spontaneously arising mammary tumour in BALB/cfC3H mice (Dexter *et al.* 1978; Heppner *et al.* 1978). The 6-thioguanine-resistant 4T1 tumour metastasizes via the haematogenous route to liver, lungs, bone and brain, making it a good model of human metastatic breast cancer (Heppner *et al.* 2000). 4T1 grows progressively and causes a uniformly lethal disease, even after excision of the primary tumour (Morecki *et al.* 1998,; Pulaski *et al.* 2000). In the present study, we have demonstrated that the 4T1 tumour induces a leukemoid reaction with splenomegaly following orthotopic transplant into the mammary fatpads of female BALB/c mice. Using flow cytometry, we have characterized the myeloid cells infiltrating primary tumours and metastatic organs. We also have shown that the 4T1 tumour constitutively expresses mRNA for the myeloid cell chemokines MCP-1, KC, RANTES, MIP-1α and MIP-1β that may be responsible for both the leukemoid reaction and myeloid cell infiltrations.

Materials and methods

Mice

Six- to eight-week-old, female BALB/c mice (15–25 g) were obtained from the Charles River Laboratories/NIH (Wilmington, MA, USA). The mice were housed in a ventilated barrier rack (Lab Products, Inc., Seaford, DE, USA) in a temperature-controlled facility on a 12-h photoperiod. The mice were given food and water *ad libitum*. This research was conducted under a protocol approved by the University of Nevada, Reno Institutional Animal Care and Use Committee.

Tumour cell culture

The 4T1 mouse mammary carcinoma was obtained from the American Type Culture Collection (Rockville, MD, USA). The 6-thioguanine-resistant cells were grown in RPMI 1640 medium supplemented with 10% fetal bovine serum (both from Hyclone, Logan, UT, USA), plus 1.0 mM sodium pyruvate, and 100 U/ml penicillin, and 100 μg/ml streptomycin (all from Cambrex, Walkersville, MD, USA). In one experiment, tumour cells were cultured overnight with 1 ng/ml recombinant mouse IFN-γ (>1.0×10^7 units/mg) (Chemicon, Temecula, CA, USA).

Measurement of tumour growth

Mice were injected in the mammary fatpad with 1.0×10^4 early passage 4T1 cells harvested from culture by treatment with 0.25% trypsin. Tumour growth was assessed morphometrically using electronic calipers, and tumour volumes were calculated according to the formula V (mm^3) = L (major axis) x W^2 (minor axis)/2 (Carlsson *et al.* 1983). Experiments were terminated when the tumours reached an average diameter of 16 mm or when mice became moribund.

Enzymatic digestion of primary tumours and metastatic target organs

Tumours, lungs and livers were excised and surface blood was removed by rinsing in Hanks' Buffered Salt Solution (HBSS). The tumours and organs were minced with scissors in 2.5 ml HBSS, then cells and fragments were added to 2.5 ml filter-sterilized enzyme cocktail. All enzymes were purchased from Sigma (St Louis, MO, USA). Primary tumours were digested in collagenase type I (10 mg/ml) for 1 h at 37 °C on a platform rocker. The lungs were digested in 10 mg/ml collagenase type IV to which 30 units elastase had been added directly before use. Lung samples were placed at 4 °C for 75 min on a platform rocker. Livers were digested in a mixture of 10 mg/ml collagenase type I and 10 mg/ml hyaluronidase for 20–30 min at 37 °C on a platform rocker. Spleens were dissociated by mechanical disruption and sieving through 70-μm cell strainers from BD Biosciences (Bedford, MA, USA).

Clonogenic metastasis assays

To quantify spontaneous metastasis of 4T1 to liver and lungs, organs were removed, digested as described above, filtered through 70-μm cell strainers and washed two times with 1× HBSS. Cells were resuspended in medium containing 60 μM 6-thioguanine (Sigma) and serially diluted in 6-well tissue culture plates. After 10–14 days, plates were fixed with methanol and 6-thioguanine-resistant colonies were stained with 0.03% methylene blue and counted. After accounting for dilution factors, data were expressed as total number of metastatic colonies per organ.

Flow cytometry

Tumour, lung and liver cells were prepared as described above to obtain single cell suspensions. Cells were incubated for 30 min with anti-CD16/32 (Fc block) to decrease non-specific binding of immunoglobulins. The monoclonal

antibodies listed in Table 1 were used in these studies. These antibodies were diluted with staining buffer and 50 μl aliquots of 2×10^7 cells/ml suspensions were added to tubes containing no antibodies or 10 μl of various diluted antibodies. After a final wash, the cells were examined with a four-colour Beckman-Coulter XL/MCL Flow Cytometer (Beckman-Coulter, Hialeah, FL, USA). The instrument was thresholded on forward angle light scatter and signals from low angle forward light scatter (FS), orthogonal light scatter (SS) and four colors of fluorescence (FL1, FL2, FL3, FL4) were collected using logarithmic amplification. The optical filters were set to collect approximately 525 nm (FL1, fluorescein), approximately 575 nm PE (FL2, PE), approximately 670 nm (FL3, PC5) and >740 nm (FL4, PC7). Data files were analysed and median fluorescence intensities were determined with FLOWJO software (Tree Star, Inc., Ashland, OR, USA).

Gating strategies in our four-colour flow cytometric analyses of primary tumours and metastatic organs were based first on separating tumour cells (and stromal or parenchymal cells) from infiltrating haematopoietic cells. This separation procedure was done on the basis of $CD45^+$ staining, so all staining tubes included this antibody. Tumours always contain dead cells and debris, and we endeavored to exclude this small forward and side scatter material. Depending on the availability of specific fluorochrome-labelled antibodies, we were able to examine as many as four cell surface markers on the same cells. Gating strategies for dot plots were based on analysis of isotype control patterns for each marker, and gates were chosen that excluded most non-specific levels of staining. By using consistent gating, we believe that valid comparisons of tumours at different days post-transplant, and metastatic organs compared with organs from control mice, can be made. In one experiment, $CD45^+$ cells were depleted from *ex vivo* primary tumours cell suspensions using antibody-coated beads as previously described (Dupré & Hunter 2007).

Reverse transcriptase polymerase chain reaction (RT-PCR)

Total mRNA was isolated from 4T1 cells grown in culture and from digested single cell suspensions of *ex vivo* primary tumour and lung, with the ExpressDirect mRNA capture and RT system from Pierce (Rockford, IL, USA), according to manufacturer's instructions. PCR was performed at 35–40 cycles as follows: 45 s at 94°C, 45 s at 52°C, and 1 min at 72°C. PCR products were separated on 1.5% agarose gels and the ethidium bromide-stained bands visualized using the Gel Doc system and QUALITY ONE software (Bio-Rad, Hercules, CA, USA). Forward and reverse primers and amplimer sizes for each gene analysed are shown in Table 2.

Histology and cell staining

Tumours and soft tissues were fixed in ExCell solution (American Master Tech Scientific, Inc., Lodi, CA, USA). Fixed samples were dehydrated and embedded in paraffin, then 7-μ sections cut, mounted on slides, and stained with haematoxylin and eosin (H&E) (Histo-Scientific Research Laboratories, Woodstock, VA, USA). Stained slides were examined with a Nikon Eclipse 400 microscope (Nikon, Melville, NY, USA), and images were captured with a Kodak DC 120 Zoom Digital Camera and processed using the Kodak Microscopy Documentation System MDS 120 (Kodak, Rochester, NY, USA).

Statistical analysis

Mean, standard deviation and Student's *t*-tests were calculated using Microsoft Excel. *P*-values of 0.05 or less were considered significant.

Results

Myeloid cells are the predominant infiltrating haematopoietic cells in 4T1 tumours

We wanted to see if the cellular landscape of the 4T1 tumour changed over time, and because we had previously observed a profound granulocytosis in 4T1 tumour-bearing mice (Dupré & Hunter 2007), to determine if infiltrating granulocytes were a prominent feature. 4T1 tumours were harvested at different times post-tumour transplant, enzymatically digested into single cell suspensions, and examined by flow cytometry for infiltrating granulocytes and other haematopoietic cell types. Although we did not have a tumour-specific marker *per se*, the 4T1 tumour *in situ* expressed several IFN-γ-inducible surface molecules, including MHC Class II. Therefore, we were able to define the tumour cells as $CD45^-MHC\ II^+$ cells with a characteristic light scatter (Figure 1a, day 20 tumour). The flow cytometric profile of a representative day 22 tumour revealed a predominant myeloid cell infiltrate characterized by a population of $CD11b^+$ cells that constituted 86% of the $CD45^+$ infiltrating cells (Figure 1b).

As CD11b is primarily expressed on myeloid cells, normal cells derived from blood, spleen, bone marrow and peritoneal washings were examined with antibodies to CD11b, Gr-1, CD11c and F4/80 (data not shown). CD11b reacted with granulocytes, monocytes and was most heavily

Table 1 Antibody reagents for flow cytometry

Reagent	Supplier	Cat. no/lot no.	Isotype	Clone
Anti-mouse CD16/32 (Fc Block)	eBioscience	14-0161-85	R-IgG2b k	93
FITC-anti-mouse CD45	eBioscience	11-0451/E000250	R-IgG2b k	30-F11
FITC-anti-mouse Gr-1 (Ly-6 G)	eBioscience	11-5931/E003725	R IgG2b	RB6-8C5
PE-anti-mouse CD4 (L3T4)	PharMingen	553730/ M075833	R IgG2b k	GK1.5
PE-anti-mouse CD11b	eBioscience	12-0112/E000173	R IgG2b k	M1/70
PE-anti-mouse CD11c	eBioscience	12-0114/E01245	H IgG	N418
PE-anti-mouse CD19	eBioscience	12-0192/ E005211	R IgG2a k	6D5
PE-anti-mouse MHC Class II (d, b not s) ($I\text{-}A^d$)	eBioscience	12-5321-82/E008130	R IgG2b k	M5/114.15.2
PE-Cy5-anti-mouse CD3ϵ	eBioscience	15-0031/ E004767	H IgG	145-2C11
PE-Cy5-anti-mouse CD45	eBioscience	15-0451/E004642	R IgG2b k	30-F11
PE-Cy5-anti-mouse Gr-1 (Ly-6G)	eBioscience	15-5931/ E004050	R IgG2b	RB6-8C5
PE-Cy7-anti-mouse CD8a (Ly-2)	PharMingen	552877/0000061910	R IgG2a k	53-6.7
PE-Cy7-streptavidin	eBioscience	25-4325/E12003	n/a	n/a
Biotin-anti-mouse F4/80	Serotec	MCA497C/010604	R IgG2b	CI;A3-1 (F4/80)

Table 2 Primers used for RT-PCR

Primer	Sequence 5'-3'	Amplimer size
KC		
Forward	AACGCTGGCTTCTGACAACA	329
Reverse	AAACACAGCCTCCCACACAT	
MCP-1		
Forward	AGGTGTCCCAAAGAAGCTGT	241
Reverse	TGCTTGAGGTGGTTGTGGAA	
RANTES		
Forward	TGGCAGGAGTGCAACAAGAA	330
Reverse	CTCAAGTTCGCTCAGCTTTCCT	
MIP1-α		
Forward	TGAAACCAGCAGCCTTTGCT	215
Reverse	ATGCAGGTGGCAGGAATGTT	
MIP1-β		
Forward	AACACCATGAAGCTCTGCGT	291
Reverse	AGCTGCTCAGTTCAACTCCA	
GAPDH		
Forward	GTGGGCCGCTCTAGGCACCAA	837
Reverse	CTCTTTGATGTCACGCACGATTTC	

expressed on macrophages. CD11c occurred at high levels on myeloid dendritic cells from the spleen but was also found at lower levels on a wide variety of cells in the spleen and bone marrow. Gr-1, which is often considered as granulocyte-specific, labelled granulocytes most brightly but also labelled monocytes and macrophages at lower levels. F4/80, the murine epidermal growth factor (EGF) module-containing mucin-like hormone receptor 1 (Emr1) (McKnight & Gordon 1998) was expressed at high levels on macrophages (Khazen *et al.* 2005), but also occurred at lower levels, primarily on monocytes. Therefore, while high levels of expression of Gr-1, CD11c or F4/80 characteristically occurred on granulocytes, dendritic cells or macrophages, respectively, many normal myeloid cells expressed lower levels of these molecules.

Among the cells recovered from the tumours, most of the $CD45^+$ cells stained with F4/80, CD11c (Figure 1c), and many of these cells also stained with the Gr-1 antibody. There was a population of $Gr\text{-}1^+$ granulocytes that did not stain for either F4/80 or CD11c, together with a Gr-1 negative population that represented lymphoid cells. $CD45^+$ tumour-infiltrating haematopoietic cells progressively increased in numbers as the tumours grew (Figure 2a). $CD11b^+$ myeloid cells were the predominant tumour-infiltrating cells (Figure 2b), increasing to >90% of $CD45^+$ cells in day 29 tumours. Lymphoid cells ($CD3^+$ and $CD19^+$) and other cells comprised less than 5% of $CD45^+$ cells in day 29 tumours.

Transcripts for the chemokines KC, MCP-1, RANTES are expressed by cultured 4T1 tumour cells, and transcripts for these chemokines and MIP-1α and MIP-1β are expressed in cells from enzymatically digested 4T1 tumours

The prominent myeloid cell infiltrates observed in primary tumours suggested that the 4T1 tumour might be making myeloid cell-specific chemokines. It has been reported that the 4T1 tumour cells *in vitro* express mRNA for the myeloid cell chemokines KC, MCP-1, RANTES, MIP-1α and MIP-1β (Kurt *et al.* 2001; Adler *et al.* 2003; Vitiello *et al.* 2004), and we wanted to verify that the 4T1 cells used in our studies also expressed the genes for these chemokines *in vitro*, and to see if these chemokines were expressed in the primary

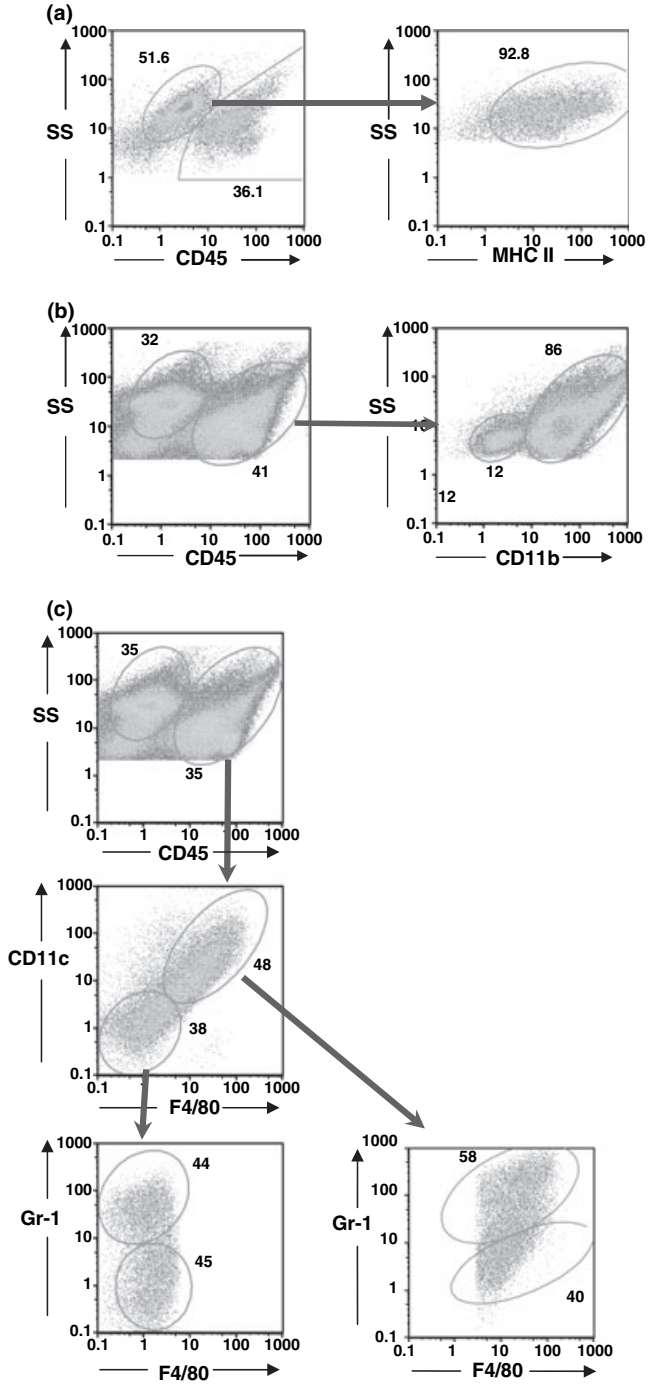

Figure 1 CD11b$^+$ myeloid cells are the predominate infiltrating cells in primary 4T1 tumours. Primary tumours were digested with an enzyme cocktail, dissociated into single cell suspensions, stained with FITC-anti-CD45 and PE-anti-I-A^d, PE-Cy5-anti-CD3e, PE-Cy5-anti-Gr-1, PE-Cy7-anti-CD8a (a), FITC-anti-Gr-1, PE-anti-CD11b, PE-Cy5-anti-CD45 (b), and PE-Cy5-anti-CD45, PE-anti-CD11c, FITC-anti-Gr-1, PE-Cy7-streptavidin, and biotin-anti-F4/80 (c), and examined by flow cytometry. (a) Tumour cells were identified as CD45$^-$/MHC II$^+$ cells (92.8% of CD45$^-$ population). (b) CD45$^+$ infiltrating cells are predominantly CD11b$^+$ myeloid cells. (c) CD45$^+$ cells stained with both F4/80 and CD11c, and many stained with Gr-1. A population of Gr-1$^+$ cells did not stain with either F4/80 or CD11c, together with a Gr-1 negative population that represented lymphoid cells.

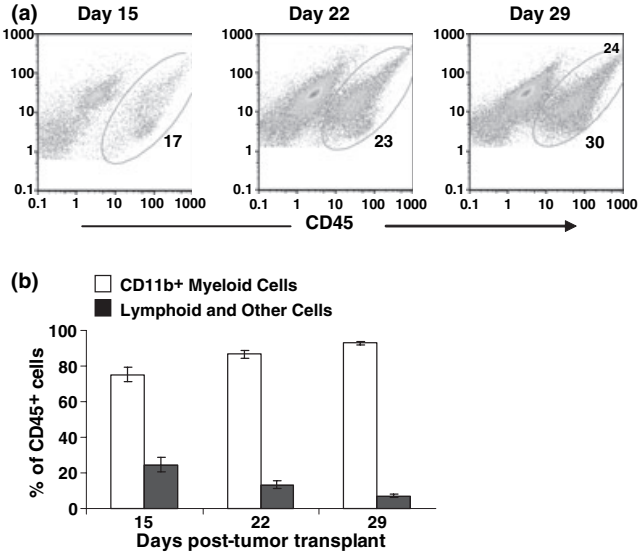

Figure 2 The cellular landscape of the 4T1 tumour changes over time. (a) Flow cytometric dot plots of CD45$^+$ tumour-infiltrating cells on days 15, 22, and 29 post-tumour transplant. (b) Single cell suspensions of primary tumour cells and infiltrates were labelled with FITC-anti-CD45, PE-anti-CD11b, PE-Cy5-anti-Gr-1, PE-Cy5-anti-CD3e and PE-Cy7-anti-CD8a. CD11b$^+$ myeloid cells and lymphoid and other cells are shown as percentages of CD45$^+$ tumour-infiltrating haematopoietic cells. Bars represent mean ± SD for groups of three mice in one of two similar experiments.

tumour *in vivo*. We found that 4T1 tumours grown *in vitro* expressed KC, MCP-1, and RANTES mRNA, and RNA extracted from the primary tumour depleted of all but 7% CD45$^+$ cells also revealed KC, MCP-1 and RANTES transcripts (Figure 3a), although non-tumour sources of these messages could not be ruled out. Transcripts for two other CC chemokines, MIP-1α and MIP-1β, were not expressed by 4T1 cells *in vitro* even in the presence of IFN-γ (data not shown), but were expressed in lysates from primary tumours (Figure 3b). These findings suggest that the myeloid cell infiltrates of primary 4T1 tumours may be caused in part by chemokines produced by tumour cells and tumour-infiltrating haematopoietic cells.

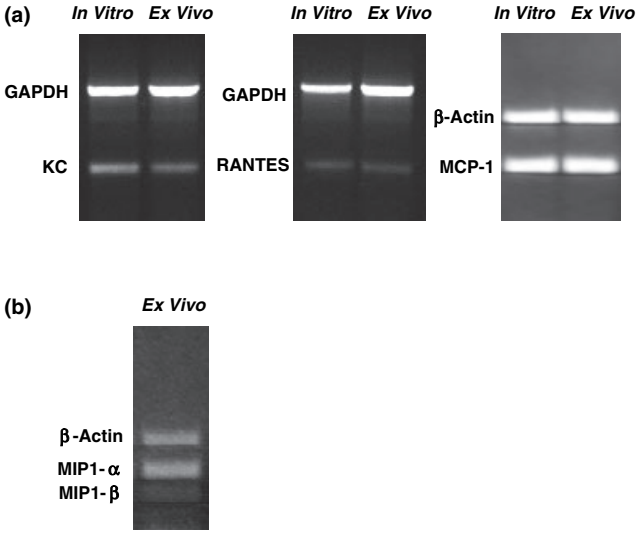

Figure 3 Chemokine mRNA expression in cultured 4T1 tumour cells and 4T1 tumour cells from primary tumours partially depleted of CD45$^+$ cells. (a) Ethidium bromide-stained 1.5% agarose gels show expression of mRNA transcripts for the myeloid cell CC chemokines KC, RANTES and MCP-1 in 1×10^6 cultured 4T1 cells and 1×10^6 cells from enzymatically digested primary tumours partially depleted of CD45$^+$ cells as described in the *Materials and methods*. (b) Expression of mRNA transcripts for the CC chemokines MIP-1α and MIP-1β in 4T1 tumour cells from enzymatically digested primary tumours partially depleted of CD45$^+$ cells as described in the *Materials and methods*.

Table 3 Numbers of clonogenic metastatic colonies at different days after tumour transplantion

	Lung	Liver
Day 8	5 (0–10)	115 (42–233)
Day 15	35 (0–123)	1,750 (211–3347)
Day 22	3750 (450–10,141)	39,768 (4,362–87,248)
Day 29	18,153 (1542–40,960)	126,880 (4,325–368,643)

All results are the mean and (range) (n = 4 or more mice per group).

Livers and lungs of mice with metastatic tumours have profound granulocytic infiltrates

The 4T1 tumour is highly metastatic, with lungs and liver as the principal target organs. To see if haematopoietic cell infiltrates were present in these organs with metastatic tumour foci, lungs and liver were harvested at different times post-tumour transplant; portions of each tissue were processed for histology and the remainder enzymatically dissociated into single cell suspensions. Some of the dissociated cells were stained with fluorochrome-labelled antibodies specific for haematopoietic cell types and examined by flow cytometry, and some were used for analysis of tumour metastases by colony forming assay. Metastases to lungs and liver were detected by day 8 post-tumour transplant, and though the data were quite variable, more metastatic tumour colonies were seen in cultures of lungs and livers from mice with more long-standing tumours (Table 3).

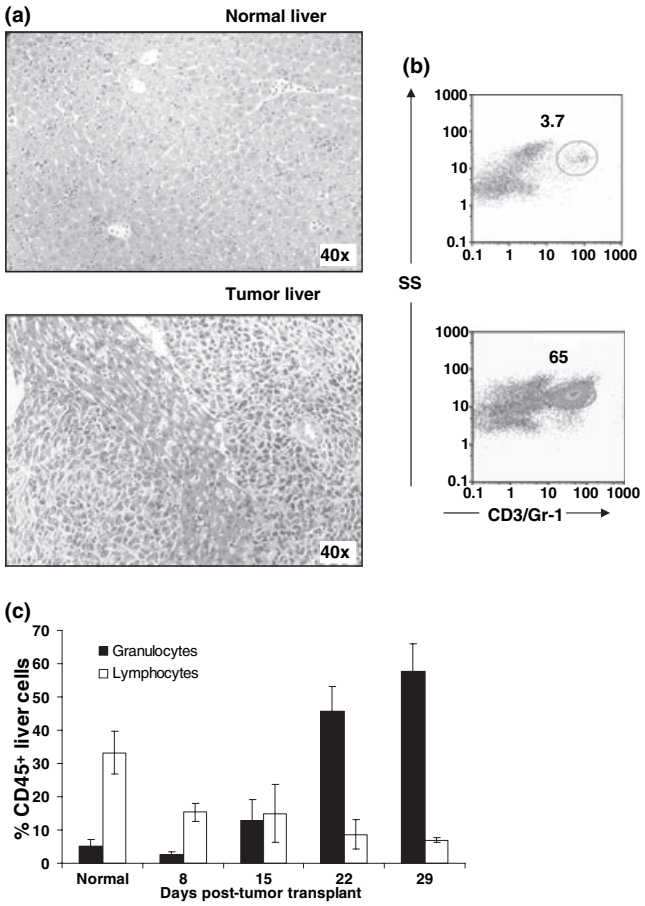

Figure 4 Granulocytic infiltrates in livers of 4T1 tumour-bearing mice. (a) H&E stained sections from livers of normal and 29-day tumour-bearing mice. (b) Bivariate flow cytometric dot plots showing the increase in infiltrating Gr-1$^+$ granulocytes in livers of tumour-bearing mice. Livers were digested with an enzyme cocktail, made into a single cell suspension, stained with FITC-anti-CD45, PE-anti-CD4, PE-anti-CD19, PE-Cy5-anti-CD3e, PE-Cy5-anti-Gr-1 and PE-Cy7-anti-CD8a, and analysed by flow cytometry. Total liver cells were first gated on CD45, and then examined for Gr-1 staining. Numbers represent Gr-1$^+$ cells as a percent of CD45$^+$ cells in the liver. (c) Granulocytes (Gr-1$^+$) and lymphocytes (CD3$^+$ T lymphocytes and CD19$^+$ B lymphocytes) as a percentage of CD45$^+$ cells in livers of normal mice and mice at different times after tumour transplantation. Bars represent mean ± SD (four mice per group) from a representative experiment.

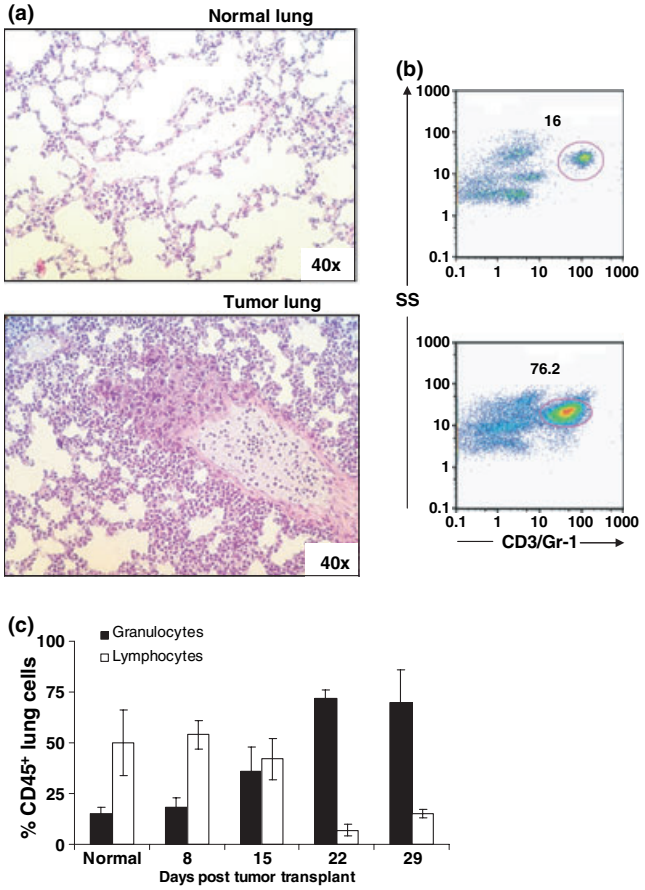

Figure 5 Granulocytic infiltrates in lungs of 4T1 tumour-bearing mice. (a) H&E stained sections from lungs of normal and 29-day tumour-bearing mice. (b) Bivariate flow cytometric dot plots showing the increase in infiltrating Gr-1$^+$ granulocytes in lungs of tumour-bearing mice. Lungs were digested with an enzyme cocktail, made into a single cell suspension, stained with FITC-anti-CD45, PE-anti-CD4, PE-anti-CD19, PE-Cy5-anti-CD3e, PE-Cy5-anti-Gr-1 and PE-Cy7-anti-CD8a, and analysed by flow cytometry. Total lung cells were first gated on CD45, then Gr-1. Numbers represent Gr-1$^+$ cells as a percent of CD45$^+$ cells. (C) Granulocytes (Gr-1$^+$) and lymphocytes (CD3$^+$ T lymphocytes and CD19$^+$ B lymphocytes) as a percentage of CD45$^+$ cells in lungs of normal mice and mice at different times after tumour transplantation. Bars represent mean ± SD (four mice per group) from a representative experiment.

Histologic examination of livers from tumour-bearing mice revealed granulocytes in the large blood vessels and sinusoids (Figure 4a). Metastatic tumour foci were seen in the normal liver parenchyma, and granulocytic infiltrates were observed about the tumour margins. Flow cytometric profiles of enzymatically dissociated liver cells from tumour-bearing mice demonstrated a significant infiltrate of Gr-1$^+$ granulocytes (Figure 4b). In livers of control mice Gr-1$^+$ granulocytes constituted <15% of CD45$^+$ cells (Figure 4c), but in 4T1 tumour-bearing mice Gr-1$^+$ cells had increased to >50% of CD45$^+$ cells by day 29 post-tumour transplant. T and B lymphocytes constituted a third of the CD45$^+$ lung cells in normal mice, but decreased to <10% in mice bearing mature tumours. Focal areas of extramedullary haematopoiesis were observed in the livers from 4T1 tumour-bearing mice as well, and most of these cells appeared to be in the myeloid series (data not shown).

The lungs of 4T1 tumour-bearing mice revealed metastatic foci with granulocytic infiltrations. The overall lung picture was one of interstitial granulocytic infiltration with almost no evidence of alveolar infiltrates (Figure 5a). As shown in the liver, flow cytometric profiles of enzymatically digested lung cells from tumour-bearing mice demonstrated a significant infiltrate of Gr-1$^+$ granulocytes (Figure 5b). These cells constituted <20% of CD45$^+$ cells in control mice, and in tumour-bearing mice Gr-1$^+$ cells progressively increased to >60% of CD45$^+$ cells 29 days post-tumour transplant. T and B lymphocytes constituted 50% of CD45$^+$ lung cells in normal mice, but in tumour-bearing mice these numbers dropped to <15%. These data indicate that livers and lungs with metastatic 4T1 tumour foci are infiltrated with large numbers of immature granulocytes.

Discussion

Analysis of the kinetics of tumour-infiltrating haematopoietic cells indicated that CD11b$^+$ myeloid cells with the F4/80$^+$CD11c$^+$ Gr-1$^+$ phenotype were the first to arrive in the tumour, along with small numbers of Gr-1$^+$/CD11c$^-$/F4/80$^-$ granulocytes, and CD4 and CD8 T cells. As tumours matured, the myeloid infiltrate increased while lymphoid cells decreased. Inaba *et al.* (1993) showed that cells of the common myeloid progenitor can have the F4/80$^+$CD11c$^+$Gr-1$^+$ phenotype, and suggested that these immature myeloid cells are capable of differentiating into macrophages, dendritic cells, or granulocytes under the influence of certain cytokines or growth factors. We have chosen to describe both the F4/80$^+$CD11c$^+$Gr-1$^+$ and the F4/80$^+$CD11c$^+$Gr-1$^-$ populations observed in the primary tumours as myeloid cells. The Gr-1$^+$CD11b$^+$ population is also heterogeneous (Fleming *et al.* 1993; Angulo *et al.* 2000; Bronte *et al.* 2000; Pelaez *et al.* 2001), and includes granulocytes, monocytes, and varying numbers of immature cells of the myelomonocytic lineage identified by another set of markers (CD31, ER-MP58, Ly-6C and ER-MP54). By the combination of Gr-1 staining, light scatter, and morphology, we have chosen to use the term granulocyte to describe the predominant population of Gr-1$^+$ myeloid cells observed in

the spleen, and organs with metastatic tumours. We also used the term granulocytes to describe the small population of Gr-1$^+$F4/80$^-$CD11$^-$ observed in the primary tumour.

It has been reported that the 4T1 tumour produces a variety of myeloid cell chemokines including MCP-1, KC, RANTES, MIP-1α and MIP-1β (Kurt *et al.* 2001; Adler *et al.* 2003; Vitello *et al.* 2004). We also demonstrated that the 4T1 tumour used in our laboratory expresses the genes for MCP-1, RANTES and KC, and although we did not demonstrate the presence of MIP-1α, and MIP-1β *in vitro*, transcripts for these chemokines were detected in RNA extracted from tumours growing *in vivo*. We had previously identified transcripts of GM-CSF in both cultured and primary tumours (Dupré & Hunter 2007), and this colony stimulating factor also serves as a granulocyte chemokine (Gomez-Cambronero *et al.* 2003). These data suggest that the observed myeloid cell infiltrate may be orchestrated at least in part by chemokines released by the 4T1 tumour itself, and by tumour-infiltrating haematopoietic cells.

It has been reported that the 4T1 tumour metastasizes to liver and lungs as early as 8 days post-tumour transplant (Kershaw *et al.* 2004), and this was verified in our studies (data not shown). Our clonogenic metastasis data were quite variable, as has been reported by other groups using the same assay with the 4T1 tumour (Aslakson & Miller 1992; Pulaski & Ostrand-Rosenberg 1998; Pulaski *et al.* 2002). However, there were clearly more metastatic cells in livers and lungs of mice with mature tumours. This is most likely the result of proliferation of these metastatic foci rather than continued export of metastatic cells from the primary tumour as it has been shown that metastatic foci continue to expand after excision of the primary tumour (Morecki *et al.* 1998; Pulaski *et al.* 2000).

Histologic examination of liver sections from tumour-bearing mice revealed large numbers of granulocytes in the sinusoids, and there was evidence of granulocytic infiltrations near the tumour margins. Cross-sections of blood vessels also showed large numbers of granulocytes. Small foci of extramedullary haematopoiesis were observed in the liver, and most of these cells appeared to be in the myeloid lineage (data not shown). In the lungs, discrete metastatic tumour foci were seen in the parenchyma, often growing out of a blood vessel. These tumour foci were surrounded by granulocytes, but areas of lung tissue without evidence of metastatic tumour exhibited more generalized interstitial granulocytic infiltrations. There was little evidence of granulocytes in the alveoli. It is interesting to note that the histologic profiles observed in lungs of 4T1 tumour-bearing mice were remarkably similar to that seen in the lungs of mice transduced with a retroviral construct coding for G-CSF (Johnson *et al.* 1989).

Flow cytometric analysis of livers and lungs of 4T1 tumour-bearing mice at different times after transplantation revealed a progressive increase in granulocytic infiltrates. By 29 days post-tumour transplant, granulocytes in the liver increased to 31% of total liver cells. Remarkably, in the same time frame granulocytes had increased to 81% of total lung cells. To the best of our knowledge, granulocytic infiltrates of the magnitude observed in the lungs of 4T1 mice have not been reported in other tumours.

In the present study, we have characterized the predominant myeloid cell infiltrations of primary 4T1 tumours and metastatic organs. We also have shown that the 4T1 tumour growing *in vivo* expresses genes for the CC chemokines MCP-1, KC, RANTES, MIP-1α and MIP-1β. These tumour-derived chemokines may be responsible for the observed myeloid cell infiltrations, and suggest that tumour-derived factors can sculpt the cellular landscape of the primary tumour and metastatic tumour foci.

Acknowledgements

This work was supported in part by a grant from the Henry Rushing Fund. The Flow Cytometry Core facility received support from a National Institutes of Health Biological Resources Infrastructure Grant P20 RR16464.

References

Adler E.P., Lemken C.A., Katchen N.S., Kurt R.A. (2003) A dual role for tumor-derived chemokine RANTES (CCL5). *Immunol. Lett.* **90**, 187–194.

Aeed P.A., Nakajima M., Welch D.R. (1988) The role of polymorphonuclear leukocytes (PMN) on the growth and metastatic potential of 13762NF mammary adenocarcinoma cells. *Int. J. Cancer* **42**, 748–759.

Almand B., Clark J.I., Nikitina E. *et al.* (2001) Increased production of immature myeloid cells in cancer patients: a mechanism of immunosuppression in cancer. *J. Immunol.* **166**, 678–689.

Angulo I., de las Heras F.G., Garcia-Bustos J. F., Gargallo D., Munoz-Fernandez M. A., Fresno M. (2000) Nitric oxide-producing CD11b(+)Ly-6G(Gr-1)(+)CD31(ER-MP12)(+) cells in the spleen of cyclophosphamide-treated mice: implications for T-cell responses in immunosuppressed mice. *Blood* **95**, 212–220.

Aslakson C.J. & Miller F.R. (1992) Selective events in the metastatic process defined by analysis of the sequential

dissemination of subpopulations of a mouse mammary tumor. *Cancer Res.* **52**, 1399–1405.

Borsig L., Wong R., Hynes R.O., Varki N.M., Varki A. (2002) Synergistic effects of L- and P-selectin in facilitating tumor metastasis can involve non-mucin ligands and implicate leukocytes as enhancers of metastasis. *Proc. Natl. Acad. Sci. U.S.A.* **99**, 2193–2198.

Bronte V., Wang M., Overwijk W.W. *et al.* (1998) Apoptotic death of CD8+ T lymphocytes after immunization: induction of a suppressive population of Mac-1+/Gr-1+ cells. *J. Immunol.* **161**, 5313–5320.

Bronte V., Apolloni E., Cabrelle A. *et al.* (2000) Identification of a CD11b(+)/Gr-1(+)/CD31(+) myeloid progenitor capable of activating or suppressing CD8(+) T cells. *Blood* **96**, 3838–3846.

Bronte V., Serafini P., Apolloni E., Zanovello P. (2001) Tumor-induced immune dysfunctions caused by myeloid suppressor cells. *J. Immunother.* **24**, 431–446.

Carlsson G., Ekelund L., Stigsson L., Hafstrom L. (1983) Vascularization and tumour volume estimations of solitary liver tumours in rats. *Ann. Chir. Gynaecol.* **72**, 187–191.

Colombo M.P., Ferrari G., Stoppacciaro A. *et al.* (1991) Granulocyte colony-stimulating factor gene transfer suppresses tumorigenicity of a murine adenocarcinoma in vivo. *J. Exp. Med.* **173**, 889–897.

Colombo M.P., Lombardi L., Melani C. *et al.* (1996) Hypoxic tumor cell death and modulation of endothelial adhesion molecules in the regression of granulocyte colony-stimulating factor-transduced tumors. *Am. J. Pathol.* **148**, 473–483.

Coussens L.M. & Werb Z. (2001) Inflammatory cells and cancer: think different!. *J. Exp. Med.* **193**, F23–F26.

Dexter D.L., Kowalski H.M., Blazar B.A., Fligiel Z., Vogel R., Heppner G.H. (1978) Heterogeneity of tumor cells from a single mouse mammary tumor. *Cancer Res.* **38**, 3174–3181.

Di Carlo E., Forni G., Lollini P., Colombo M.P., Modesti A., Musiani P. (2001) The intriguing role of polymorphonuclear neutrophils in antitumor reactions. *Blood* **97**, 339–345.

Dupré S. & Hunter K.W. Jr (2007) Murine mammary carcinoma 4T1 induces a leukemoid reaction with splenomegaly: association with tumor-derived growth factors. *Exp. Mol. Pathol.* **82**, 12–24.

Fleming T.J., Fleming M.L., Malek T.R. (1993) Selective expression of Ly-6G on myeloid lineage cells in mouse bone marrow. RB6-8C5 mAb to granulocyte-differentiation antigen (Gr-1) detects members of the Ly-6 family. *J. Immunol.* **151**, 2399–2408.

Gomez-Cambronero J., Horn J., Paul C.C., Baumann M.A. (2003) Granulocyte-macrophage colony-stimulating factor is a chemoattractant cytokine for human neutrophils: involvement of the ribosomal p70 S6 kinase signaling pathway. *J. Immunol.* **171**, 6846–6855.

Heppner G.H., Dexter D.L., DeNucci T., Miller F.R., Calabresi P. (1978) Heterogeneity in drug sensitivity among tumor cell subpopulations of a single mammary tumor. *Cancer Res.* **38**, 3758–3763.

Heppner G.H., Miller F.R., Shekhar P.M. (2000) Nontransgenic models of breast cancer. *Breast Cancer Res.* **2**, 331–334.

Inaba K., Inaba M., Deguchi M. *et al.* (1993) Granulocytes, macrophages, and dendritic cells arise from a common major histocompatibility complex class II-negative progenitor in mouse bone marrow. *Proc. Natl. Acad. Sci. U.S.A.* **90**, 3038–3042.

Johnson G.R., Gonda T.J, Metcalf D., Hariharan I.K., Cory S. (1989) A lethal myeloproliferative syndrome in mice transplanted with bone marrow cells infected with a retrovirus expressing granulocyte-macrophage colony stimulating factor. *EMBO J.* **8**, 441–448.

Kershaw M.H., Jackson J.T., Haynes N.M. *et al.* (2004) Gene-engineered T cells as a superior adjuvant therapy for metastatic cancer. *J. Immunol.* **173**, 2143–2150.

Khazen W., M'Bika J.P., Tomkiewicz C. *et al.* (2005) Expression of macrophage-selective markers in human and rodent adipocytes. *FEBS Lett.* **579**, 5631–5634.

Kurt R.A., Baher A., Wisner K.P., Tackitt S., Urba W.J. (2001) Chemokine receptor desensitization in tumor-bearing mice. *Cell Immunol.* **207**, 81–88.

Kusmartsev S. & Gabrilovich D.I. (2002) Immature myeloid cells and cancer-associated immune suppression. *Cancer Immunol. Immunother.* **51**, 293–298.

McKnight A.J. & Gordon S. (1998) The EGF-TM7 family: unusual structures at the leukocyte surface. *J. Leukoc. Biol.* **63**, 271–280.

Morecki S., Yacovlev L., Slavin S. (1998) Effect of indomethacin on tumorigenicity and immunity induction in a murine model of mammary carcinoma. *Int. J. Cancer* **75**, 894–899.

Pekarek L.A., Starr B.A., Toledano A.Y., Schreiber H. (1995) Inhibition of tumor growth by elimination of granulocytes. *J. Exp. Med.* **181**, 435–440.

Pelaez B., Campillo J.A., Lopez-Asenjo J.A., Subiza J.L. (2001) Cyclophosphamide induces the development of early myeloid cells suppressing tumor cell growth by a nitric oxide-dependent mechanism. *J. Immunol.* **166**, 6608–6615.

Pulaski B.A. & Ostrand-Rosenberg S. (1998) Reduction of established spontaneous mammary carcinoma metastases following immunotherapy with major histocompatibility complex class II and B7.1 cell-based tumor vaccines. *Cancer Res.* **58**, 1486–1493.

Pulaski B.A., Clements V.K., Pipeling M.R., Ostrand-Rosenberg S. (2000) Immunotherapy with vaccines combining MHC class II/CD80+ tumor cells with interleukin-12 reduces established metastatic disease and stimulates immune effectors and monokine induced by interferon gamma. *Cancer Immunol. Immunother.* **49**, 34–45.

Pulaski B.A., Smyth M.J., Ostrand-Rosenberg S. (2002) Interferon-gamma-dependent phagocytic cells are a critical component of innate immunity against metastatic mammary carcinoma. *Cancer Res.* **62**, 4406–4412.

Serafini P., De Santo C., Marigo I. *et al.* (2004) Derangement of immune responses by myeloid suppressor cells. *Cancer Immunol. Immunother.* **53**, 64–72.

Tabuchi T., Soma T., Yonekawa M., Komai T., Hashimoto T., Adachi M. (1992) Reduction of VX2 transplanted tumor by granulocyte depletion using extracorporeal circulation on rabbit models. *Anticancer Res.* **12**, 795–798.

Vitiello P.F., Shainheit M.G., Allison E.M., Adler E.P., Kurt R.A. (2004) Impact of tumor-derived CCL2 on T cell effector function. *Immunol. Lett.* **91**, 239–245.

Welch D.R., Schissel D.J., Howrey R.P., Aeed P.A. (1989) Tumor-elicited polymorphonuclear cells, in contrast to "normal" circulating polymorphonuclear cells, stimulate invasive and metastatic potentials of rat mammary adenocarcinoma cells. *Proc. Natl. Acad. Sci. U. S. A.* **86**, 5859–5863.

Wu Q.D., Wang J.H., Condron C., Bouchier-Hayes D., Redmond H.P. (2001) Human neutrophils facilitate tumor cell transendothelial migration. *Am. J. Physiol. Cell Physiol.* **280**, C814–C822.